J Fail. Anal. and Preven. (2013) 13:771–778
DOI 10.1007/s11668-013-9747-5

TECHNICAL ARTICLE—PEER-REVIEWED

Multi-objective Optimization of Sheet Metal Forming Die Using Genetic Algorithm Coupled with RSM and FEA

Parviz Kahhal · Seyed Yousef Ahmadi Brooghani · Hamed Deilami Azodi

Submitted: 24 April 2013 / in revised form: 26 August 2013 / Published online: 28 September 2013

Abstract Present study describes the approach of applying response surface methodology (RSM) with a Pareto-based multi-objective genetic algorithm to assist engineers in optimization of sheet metal forming. In many studies, finite element analysis and optimization technique have been integrated to solve the optimal process parameters of sheet metal forming by transforming multi-objective problem into a single-objective problem. This paper aims to minimize objective functions of fracture and wrinkle simultaneously. Design variables are blank-holding force and draw-bead geometrical parameters (length and diameter). RSM has been used for design of experiment and finding relationship between variables and objective functions. Forming limit diagram has been used to define objective functions. Finite element analysis applied for simulating the process. Proposed approach has been investigated on a fuel tank drawing part and it has been observed that it is more effective and accurate than traditional finite element analysis method and the "trial and error" procedure.

Keywords Multi-objective optimization · Sheet metal forming · Response surface model · Pareto front · Genetic algorithm · Forming limit diagram

P. Kahhal (✉) · S. Y. A. Brooghani
Faculty of Engineering, University of Birjand, Birjand, Iran
e-mail: parviz_pkl@yahoo.com

H. D. Azodi
Faculty of Mechanical Engineering, Arak University of Technology, Arak, Iran

Introduction

In recent years, numerical simulation of sheet metal forming has become an important tool to check the manufacture feasibility of the deep drawing process and the preliminary design of new stamped parts with more and more complex 3D geometry. Finite element modeling (FEM) has the advantage to reduce the production cost by predicting the defects in the part such us: spring-back, rupture, wrinkling, buckling, shape errors, and optimizing the process parameters.

However, in order to achieve good product quality and process reliability, the procedure of Finite Element Analysis (FEA) has to be performed "by hand" many times with different combinations of process parameters. Meanwhile, it is very difficult for engineers to consider so many parameters for a complex problem, since FEA procedure is very time-consuming and relies much on the users' experience. So, under the needs of reduction on design time, reduction on development cost, and reduction on parts weight, there is an urgent need for more efficient and accurate method in order to improve the current design situation.

In this respect, Makinouchi [1] used FEM to predict the defects of fracture, wrinkling, and springback of the sheet successfully. Many researchers have used numerical simulation with optimization methods to optimize the sheet metal forming. Ohata et al. [2] optimized process condition by integrating the sweeping simplex method and finite element analysis to achieve a uniform thickness distribution. Guo et al. [3] combined the inverse approach (IA) and a sequential quadratic programming method to optimize the blank shape. Naceur et al. [4] also used the IA to optimize drawbead restraining forces in order to improve the sheet metal formability in deep drawing process. Kayabasi and Ekici [5] integrated finite element analysis,

response surface methodology (RSM), and genetic algorithm (GA) to improve formability of an automobile side panel. Chen et al. [6] investigated the influence of different blank holder gaps and shell element types on formability of a washing-trough and optimized the process. Azaouzi et al. [7] developed an automatic numerical procedure based on commercial FEM code and heuristic optimization algorithms for the blank shape design of high precision metallic parts. Khalili et al. [8] combined reduced basis technique and RSM to optimize initial blank shape. Huang et al. [9] used combination of FEM and the RSM to optimize the intermedial tool surfaces and therefore minimize the thickness variation in multi-step sheet metal stamping. Ohata et al. [10] used RSM to find the annealing conditions suitable for a sheet forming condition. Hu et al. [11] used adaptive response surface (RS) based on intelligent sampling method for optimization of initial blank shape and blank hold force in sheet forming process.

Most problems in nature have several (possibly conflicting) objectives to be satisfied. Many of these problems are frequently treated as single-objective optimization problems by transforming all but one objective into constraints.

It is obvious that the sheet metal forming is a multi-objective problem with conflicting relationships between multiple objective functions which many researches have been done in this area. Jansson and Nilsson [12] used RSM and space mapping technique to optimize draw-in for an automotive sheet metal part. Later Janssen et al. [13] used a design hierarchy and RSM to avoid failure in the material and at the same time reach an acceptable through thickness strain. Guangyong et al. [14] optimize restraining forces and geometric parameters of drawbead by integrating the six sigma principle, dual RSM and a multiobjective particle swarm optimization.

Previous studies solved the multi-objective optimization problem (MOOP) of sheet metal forming by transforming the problem into a single-objective optimization problem, such as the weight coefficients approach which combined multiple objective functions into one. Unfortunately, it is a big trouble for users to determine the value of these coefficients, although these coefficients are crucial for the results of optimization. Another problem is that each set of coefficient combination can only acquire one optimal solution, and it is hard to make sure whether the solution achieved is an optimal one or not.

However, in engineering design domains, more and more attentions have been drawn to multi-objective genetic algorithm (MOGA), which mimics the natural selection process in which a superior creature evolves while inferior creatures fade out from their population as generations go by [15–17].

Many advantages of MOGA are very attractive [18], such as the capability of exploring a large design space and the merit of none gradients information is needed. But, the most important one is MOGA that can compute multiple independent objective functions simultaneously in one optimization run without converting multiple objective functions into a single objective by weighted linear combination. For these reasons, MOGA can be used for higher non-linear MOOPs such as sheet metal forming.

Some researches have been conducted, using MOGA with good results like Liu and Yang [19], although they replaced the geometry of drawing beads with restraining forces, which is not practical in most of the experimental works.

In this paper, "Multi-objective Optimization Model" section will study the design of multi-objective optimization model, "Multi-objective Optimization Algorithm" section will focus on the procedure of MOGA, "Case Study" section will discuss on case study, and "Results" and "Conclusion" sections will investigate the results and conclusion of this methodology.

Multi-objective Optimization Model

The aim of the optimization is to get the best combination of process parameters or geometry design variables which will lead to a desired sheet metal part without any defects due to fractures and wrinkles. The optimization process of sheet metal forming can be formulated as:

$$\text{Minimize} \quad F(X) = (f_1(x_1), f_2(x_2), \ldots, f_j(x_i)), \quad j = 1, 2, \ldots, m \qquad \text{(Eq 1)}$$

$$\text{Subject to} \quad b_i^{\text{lower}} \le x_i \le b_i^{\text{upper}}, \quad i = 1, 2, \ldots, n \qquad g_k(x_i) \le 0, \quad k = 1, 2, \ldots, p \qquad \text{(Eq 2)}$$

where x_i is the ith design variable, b_i^{lower} and b_i^{upper} represent the lower and upper boundary of x_i, $f_j(x_i)$ is the jth objective function of x_i and $g_k(x_i)$ is the kth constraint function of x_i [19].

Design Variables

For sheet metal forming, blank-holding force (BHF) and draw-bead geometrical parameters [radii (DBR123 and DBR456) and lengths (DBL1 and DBL23)] are very effective in formability, because the use of BHF and draw-beads on blank-holder can provide uniform pressure to restrain the blank flow into the die. Therefore, BHF, DBR123, DBR456, DBL1, and DBL23 will be considered as design variables in this study.

Objective Functions

In order to avoid the occurrence of forming defects, criteria on these forming defects were defined to judge the formability of sheet metal parts. In this study, the objective functions were calculated based on the value of these criteria for the optimization. According to the results of FEA, the strain values of elements on the drawing part were used to calculate the value of these criteria, as explained in the following.

Fracture

When the major strains of some elements lie above the forming limit curve (FLC, line $\varphi(\varepsilon_2)$), fracture may occur in this area of the part, and a higher value of the distance indicates a higher fracture tendency (Fig. 1). In this work, the squares of the distances for all elements were added to be the objective function of fracture, just as shown in the following equation:

$$\mathrm{Obj_f} = \begin{cases} \sum_{i=1}^{n} (d_{\mathrm{f}}^i)^2 = \sum_{i=1}^{n} (\varepsilon_1^i - \varphi(\varepsilon_2^i))^2 & \varepsilon_1^i > \varphi(\varepsilon_2^i) \\ 0 & \varepsilon_1^i \le \varphi(\varepsilon_2^i) \end{cases}. \quad \text{(Eq 3)}$$

In this research, FLC has been obtained by experimental tests on sheet.

Wrinkle

Similarly, when the major strains of some elements lie below the wrinkle limit curve (WLC, line $\psi(\varepsilon_2)$), wrinkle may occur in this area of the part, and a higher value of the distance indicates a higher wrinkle tendency. So, wrinkle criteria were defined by the distance from the major strain of each element to their WLC. The squares of the distances for all elements were added to be the objective function of wrinkle, just as shown in the following equation:

$$\mathrm{Obj_w} = \begin{cases} \sum_{i=1}^{n} (d_{\mathrm{w}}^i)^2 = \sum_{i=1}^{n} (\varepsilon_1^i - \psi(\varepsilon_2^i))^2 & \varepsilon_1^i > \psi(\varepsilon_2^i) \\ 0 & \varepsilon_1^i \le \psi(\varepsilon_2^i) \end{cases}. \quad \text{(Eq 4)}$$

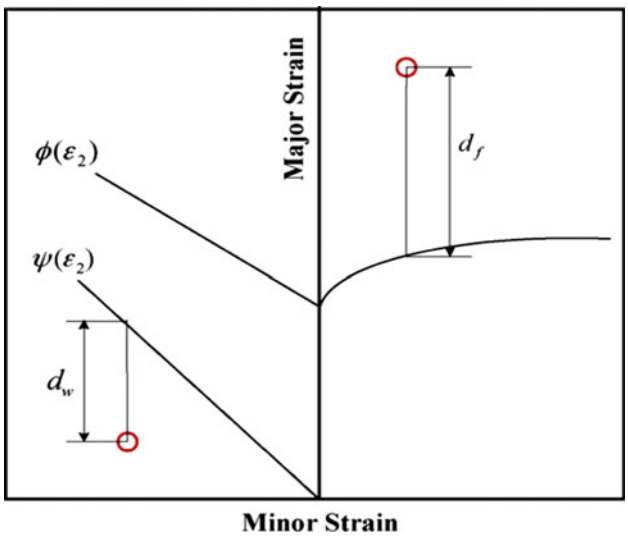

Fig. 1 Schematic diagram of objective functions definition [19]

Multi-objective Optimization Algorithm

Sheet metal forming is a multi-objective problem. In these cases, it is difficult to minimize or maximize all the objective functions simultaneously when objective functions are in trade-off relationship. In this paper, RSM has been used for the design of experiment (DOE), and GA and Pareto front have been combined to perform the optimization.

In normal GA, we take a population of genomes (individuals) randomly scattered across state space and evaluate the fitness of the results. The bests are then retained (selection), and a new population is created (reproduction), incorporating mutation and crossover operations to gain a different set of possibilities (variation). Over many generations, the population will search the state space and hopefully converge on the best solution, that is the global optimum.

In MOGA, we do much the same, except that in this case, we are trying to optimize not for one fitness parameter but against a collection of them. To achieve this, we must generate an understanding of the overall fitness of the set of objectives, so that we can compare solutions, and there are many ways of doing this. For that purpose, Pareto optimal solution has been used.

For minimum problem, a feasible solution x^* is a Pareto optimal solution if and only if, there is no other feasible solution x like that

$$f_i(x) \le f_i(x*) \quad i = 1, 2, \ldots, n. \quad \text{(Eq 5)}$$

And for at least one j, $1 \le j \le n$, satisfying

$$f_j(x) < f_i(x*). \quad \text{(Eq 6)}$$

For Example, as shown in Fig. 2, The boxed points represent feasible choices, and smaller values are preferred to larger ones. Point C is not on the Pareto solution because it is dominated by both point A and point B. Points A and B are not strictly dominated by the other one, and hence do lie on the frontier.

Procedure of Optimization

The procedure of the MOGA can be described as follows:

Step 1: Select an exchange strategy, initialize population, clear the Pareto set, make $i = 0$, and set the parameters;

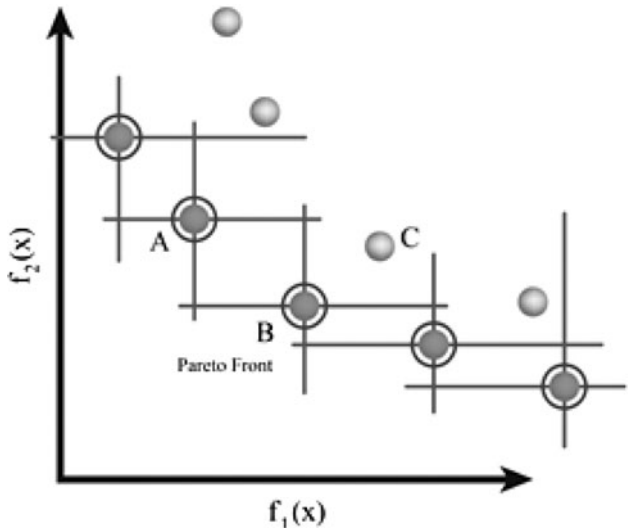

Fig. 2 Pareto optimal solution [17]

Step 2: Combine the current population with the parent population, and sort the combined population by using no dominated sorting method;
Step 3: Update the Pareto set;
Step 4: Calculate the fitness values of the individuals according to the sorting result;
Step 5: Judge whether the termination criterion is satisfied.

Response Surface Model

RSM are primarily relevant when the decision-maker desires: (1) to create a relatively accurate prediction of engineered system input and output relationships and (2) to "tune" or optimize thoroughly of the system being designed. Since these methods require more runs for a given number of factors than screening using fractional factorials, they are generally reserved for cases in which the importance of all factors is assumed, perhaps because of previous experimentation. In many RSM applications, either linear or quadratic polynomials are assumed to accurately model the observed response values. Although this is certainly not true for all cases, RSM becomes prohibitively expensive when cubic and higher-order polynomials are chosen for experiments involving several variables. In addition, cubic and higher-order polynomial models may contain one or more inflection points. In gradient-based numerical optimization schemes, the optimizer may converge to an inflection point rather than to a local or global optimum.

If n_s analyses are conducted and $p = 1, 2, \ldots, n_s$, then a quadratic RS model has the form:

$$y^{(p)} = c_o + \sum_{1 \le j \le n_v} c_j x_j^{(p)} + \sum_{1 \le j \le k \le n_v} c_{(n_v-1+j+k)} x_j^{(p)} X_k^{(p)}, \quad \text{(Eq 7)}$$

where $y^{(p)}$ is the response; $x_j^{(p)}$ and $X_k^{(p)}$ are the n_v design variables; and c_o; c_j; and $c_{(n_v-1+j+k)}$ are the unknown polynomial coefficients. Note that there are $n_t = (n_v + 1)(n_v + 2) = 2$ coefficients (i.e., model terms) in the quadratic polynomial.

However, the buildings of these surrogate models need some samples in order to construct RS to fit the true drawing process, and these samples could be produced by the DOE methods, such as space filling design (i.e., Halton sequence, latin hypercube design, Taguchi methods), classical design (i.e., Box-Behnken, full factorial), and optimal design (i.e., D-optimal, V-optimal and A-optimal designs). DOE has been a very useful tool to design and analyze complicated industrial design problems and can be helpful to understand process characteristics and investigate how inputs affects responses based on statistical backgrounds. In addition, it can be used to systematically determine the optimal process parameters with fewer testing trails.

In this study, the V-optimal design (which minimizes the average variance of the parameters and reduces the asphericity of the confidence ellipsoid) has been used for DOE and a quadratic model has been used for building RSM model.

Case Study

FEA Model

In order to improve the reliability of optimization, incremental-based dynamic explicit finite element code was selected to simulate sheet metal forming process. In this study, a fuel tank part was studied to be a case, and the FEA model is presented in Fig. 3. The material of sheet was taken Steel ST14. Plastic behavior and strain hardening have been determined by Tensile Testing which true stress–strain curve is shown in Fig. 4. Specifications of the investigated blank are presented in Table 1.

FLC for fracture criteria has been determined by experimental out-of-plane tests. For that purpose, a grid of circles has been printed photographically on a sheet. Usually, the circles are 5 mm in diameter. The specimens have been stretched over a hemispherical dome until a local neck is first observed. To achieve various strain paths, the lubrication and specimen width have been varied and eight specimens have been stretched. Full-width specimens deforming balanced biaxial tension and very narrow strips

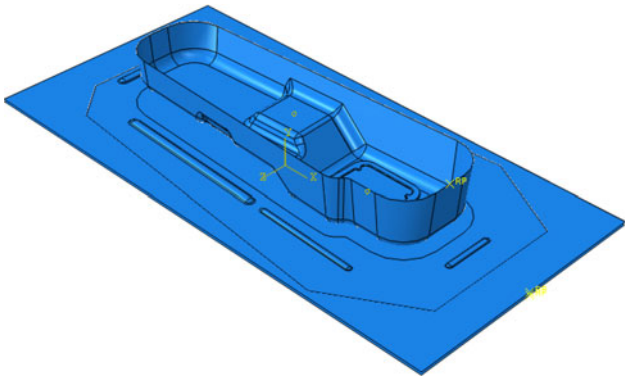

Fig. 3 FEA model of fuel tank part

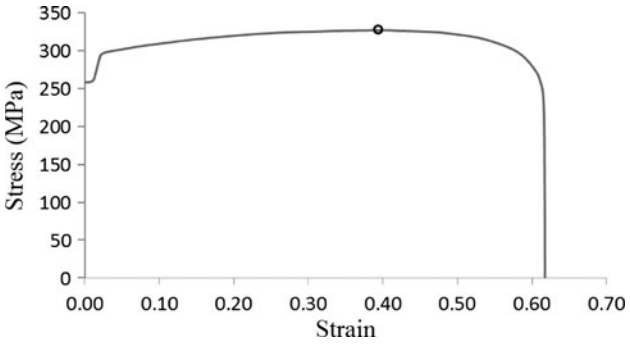

Fig. 4 True stress–strain of ST14

Table 1 Material properties of ST14

Young's modulus, GPa	200
Poisson's ratio	0.3
Yield strength, MPa	185
UTS, MPa	327

are almost in uniaxial tension [20]. Sketch of the hemispherical punch and used die are shown in Fig. 5.

Totally, 36705 linear triangular shell elements have been used to simulate the forming process. The tools were considered as rigid objects without any elastic deformation. The holder moved from up to the die with speed 7 m/s and stopped, then the punch began to move down with speed 4 m/s. ABAQUS/CAE code has been used for analysis.

Optimization Model

In order to optimize the formability of the deep drawing process, BHF and draw-bead geometrical parameters were selected to be design variables, as shown in Fig. 6. The optimization problem can be formulated as a non-linear model in the following form:

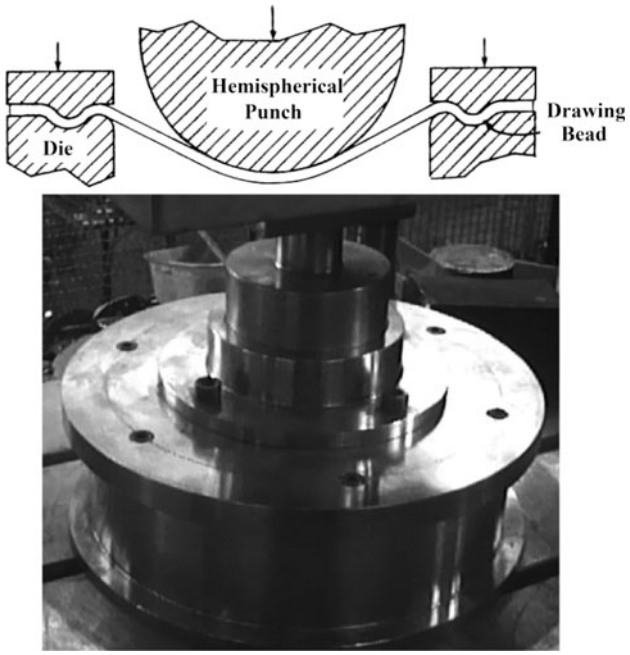

Fig. 5 Hemispherical punch and out-of-plane test die

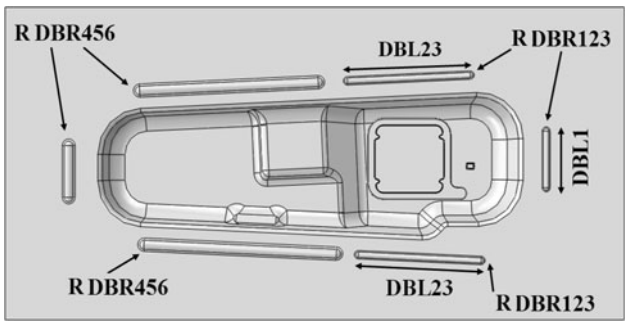

Fig. 6 Draw-bead's geometrical parameters

$$\text{Minimize} \quad F(x) = (Obj_{\text{w}}, Obj_{\text{f}}) \qquad \text{(Eq 8)}$$

Subject to:

$$\begin{aligned} &2000 \leq \text{BHF} \leq 3000 \ (\text{kN}) \\ &15 \leq \text{DBR123} \leq 25 \ (\text{mm}) \\ &15 \leq \text{DBR456} \leq 25 \ (\text{mm}) \\ &100 \leq \text{DBL1} \leq 150 \ (\text{mm}) \\ &270 \leq \text{DBL23} \leq 330 \ (\text{mm}) \end{aligned} \qquad \text{(Eq 9)}$$

Optimization procedure

Figure 7 shows the flow diagram of optimization procedure which was divided into five steps:

Step 1: Initializing model: the FEM and optimization model were both setup for their initial conditions, and following parameters were set to the MOGA model. (1)

Population size $P = 75$; (2) crossover probability $P_c = 0.8$; (3) mutation probability $P_m = 0.01$; (4) migration fracture $P_g = 0.2$; (5) Pareto front population fraction $P_p = 0.35$ (6) termination generation $T = 600$.

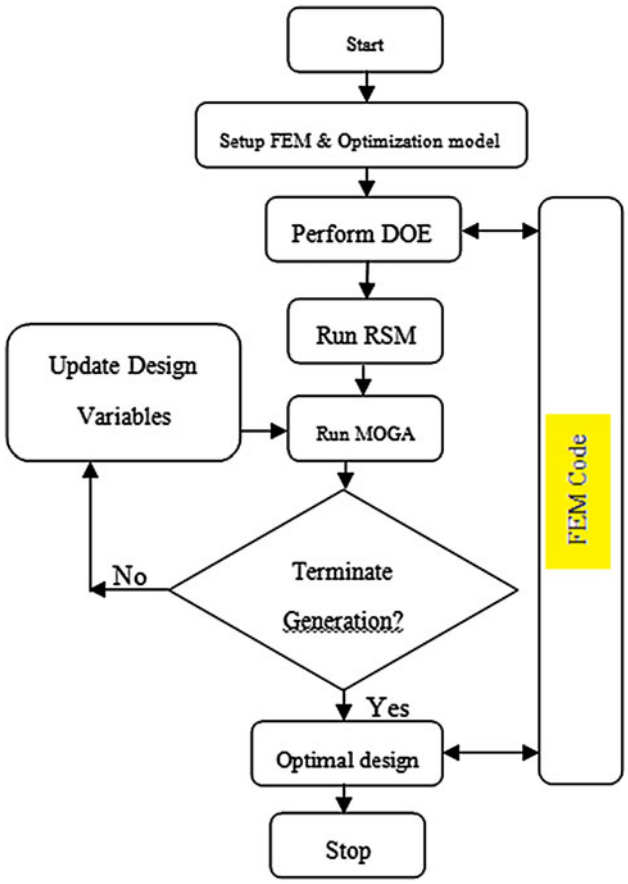

Fig. 7 Flow diagram of optimization procedure

Step 2: Performing DOE: for the construction of second-order RSM, based on DOE matrix and finite element code, each combination of design variables will be used

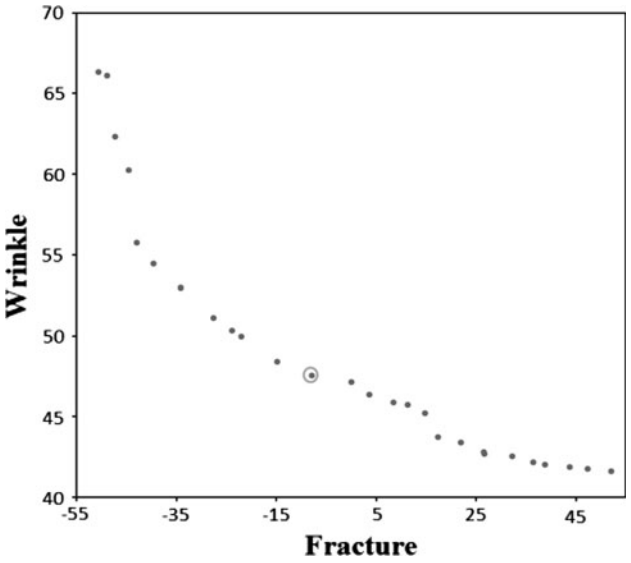

Fig. 8 Pareto optimal solutions

Table 3 Values of all design variables and objective functions

Variables	RSM (Pareto)	FEA (Pareto)
BHF, kN	2512.6348	2512.6348
DBR(123), mm	15.060442	15.060442
DBR(456), mm	15.483406	15.483406
DBR(123), mm	103.21274	103.21274
DBL(23), mm	298.14925	298.14925
Obj_f	−7.8680	0
Obj_w	47.539265	53.406506

Table 2 DOE matrix and results of FEA

#	BHF, kN	DBR(123), mm	DBR(456), mm	DBL(1), mm	DBL(23), mm	Obj_f	Obj_w
1	2000	23.667	20.333	120	330	56.182	55.696
2	2733.33	23.667	21.667	120.334	270	33.230	53.048
3	2933.333	19	25	110	270	16.908	52.215
4	2066.667	17	15	116.667	270	0.9214	57.368
5	2133.333	23	19. 667	100	330	45.668	56.719
6	2533.333	21.667	21	116.667	302	15.754	51.795
7	2400	19	23.667	150	302	2.0168	55.074
8	2933. 333	15.667	23.667	146.667	330	2.9349	48.243
9	2200	18.333	21.667	126.667	302	0.8452	56.574
10	2666.667	17.667	23	150	270	36.812	56.243
11	2333.333	15.6667	22.333	123.333	302	1.4734	51.543
12	2600	24.333	21	110	298	52.337	48.504
13	2266.667	15.667	19.667	140	330	13.410	62.905

for the running of FEA, and the objective functions will be evaluated for each point of DOE matrix. The DOE matrix and results of FEA were shown in Table 2.

Step 3: Constructing RSM: according to Eq 9, the following RS functions can be constructed based on the DOE results:

$$\begin{aligned}\mathrm{Obj_w} = {} & 539.333 + 0.2139773 \times \mathrm{BHF} + 9.324826 \\ & \times \mathrm{DBR123} - 4.228896 \times \mathrm{DBR456} + 1.434112 \\ & \times \mathrm{DBL1} - 5.932694 \times \mathrm{DBL23} - 4.510165 \\ & \times 10^{-5} \times \mathrm{BHF}^2 - 0.2378853 \times \mathrm{DBR123}^2 \\ & + 0.1133753 \times \mathrm{DBR456}^2 - 0.005676007 \\ & \times \mathrm{DBL1}^2 + 0.00999398 \times \mathrm{DBL23}^2\end{aligned} \quad \text{(Eq 10)}$$

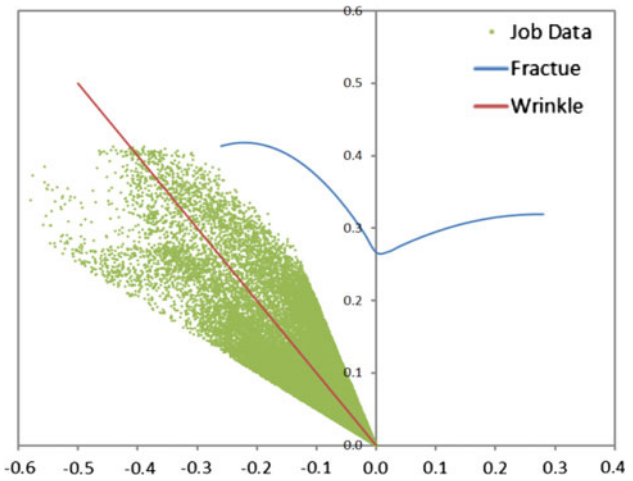

Fig. 9 FLD of fuel tank part

$$\begin{aligned}\mathrm{Obj_f} = {} & 1573.3047 - 0.45329011 \times \mathrm{BHF} - 36.204657 \\ & \times \mathrm{DBR123} + 52.3198 \times \mathrm{DBR456} - 8.9301621 \\ & \times \mathrm{DBL1} - 3.8243541 \times \mathrm{DBL23} + 8.7876935 \\ & \times 10^{-5} \times \mathrm{BHF}^2 + 0.99746368 \times \mathrm{DBR123}^2 \\ & - 1.2683234 \times \mathrm{DBR456}^2 + 0.03537017 \times \mathrm{DBL1}^2 \\ & + 0.0056372823 \times \mathrm{DBL23}^2.\end{aligned} \quad \text{(Eq 11)}$$

Step 4: Running MOGA: once the RS is constructed, the MOGA optimization technique can be used to search for the Pareto optimal solutions. The optimization procedure in this case does not have to run FEA, but uses the RSM to replace the long-time computation to evaluate the objective functions value.

Step 5: Checking termination condition: if the number of termination generation is satisfied, the optimization procedure will be terminated. If not, the process returns to Step 4.

Results

After 13 times of DOE iterations and MOGA iteration based on RSM, the Pareto optimal solutions for objectives were plotted and shown in Fig. 8, in which each point represents a Pareto optimal solution. The optimum values between objectives are conflicting with each other and there is no any point which can meet the minimized need of the two objectives simultaneously. For this study, any point may be an optimum solution, and the point shown in Fig. 8 was used as optimal solution.

Table 3 summarizes the values of all design variables and objective functions and FEA optimal values for this

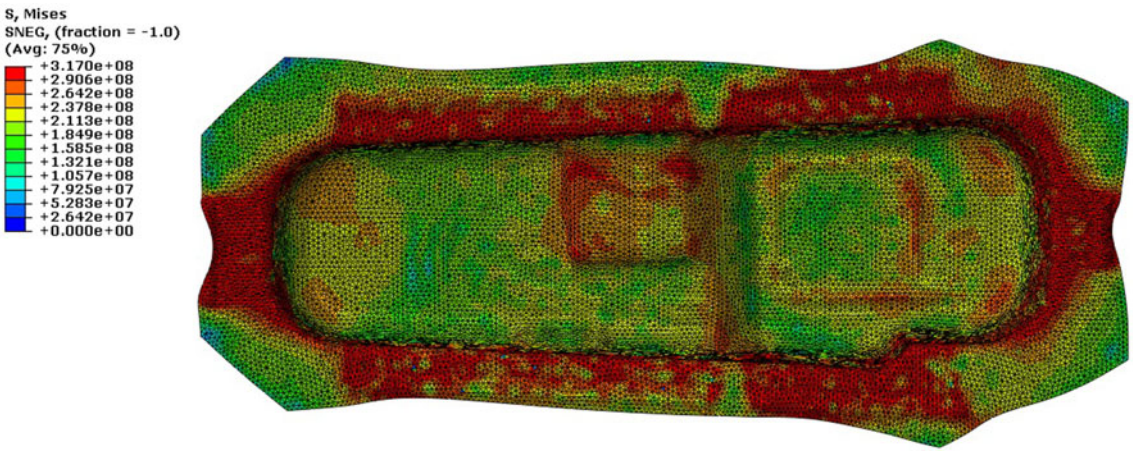

Fig. 10 Plot counter on deformed shape of fuel tank part

optimization process. From the forming limit diagram (FLD) in Fig. 9, we can find all the inside part of the die opening located in the safety region. After optimization, the value of objective function Obj_f has become zero, which means that no fractures occurred on the drawing part. Although the value of objective function Obj_w has not become zero, no wrinkles occurred inside the die opening. The cause of this matter is our definition of objective function $Obj_{w.}$

As can be seen in Fig. 10, according to optimized parameters, the fuel tank part was drawn successfully, which indicates objective functions have been reduced significantly by this optimization method.

Conclusion

Fracture and wrinkling are predominant defects in sheet metal forming process. The existence of these defects may damage surface quality, reduce dimensional precision, cause local crack of component, and lead directly to waster. In order to improve product quality and reduce cost, various optimization techniques have been successfully applied to sheet metal forming process. It has been observed that there are always conflicting relations between these objective functions, the solutions that minimize all objective are almost impossible.

It has been shown that MOGA can find all the Pareto optimal solutions by only one-time global search procedure without combining all the objectives into a single objective. So through the investigation, the proposed methodology by FEA coupled with DOE, RSM, and Pareto-based MOGA are found to be very effective in the deep drawing .The methodology shown in this paper provides the designer with more short analysis cycle time and more accurate design results than in traditional optimization methods.

The present work is all about simulation so the experiments can be done to obtain the desired product from the optimal solutions obtained by the proposed method. The present method can be further applied to design other practical drawing applications.

References

1. A. Makinouchi, Sheet metal forming simulation in industry. J. Mater. Process. Technol. **60**, 19–26 (1996)
2. T. Ohata, Y. Nakamura, T. Katayama, E. Nakamachi, K. Nakano, Development of optimum process design system by numerical simulation. J. Mater. Process. Technol. **60**, 543–548 (1996)
3. Y.Q. Guo, J.L. Batoz, H. Naceur, S. Bouabdallah, F. Mercier, O. Barlet, Recent developments on the analysis and optimum design of sheet metal forming parts using a simplified inverse approach. Comput. Struct. **78**, 133–148 (2000)
4. H. Naceur, Y.Q. Guo, J.L. Batoz, C. Knopf-Lenoir, Optimization of drawbead restraining forces and drawbead design in sheet metal forming process. Int. J. Mech. Sci. **43**, 2407–2434 (2001)
5. O. Kayabasi, B. Ekici, Automated design methodology for automobile side panel die using an effective optimization approach. Mater. Des. **28**, 2665–2672 (2007)
6. L. Chen, J.C. Yang, L.W. Zhang, S.Y. Yuan, Finite element simulation and model optimization of blankholder gap and shell element type in the stamping of a washing-trough. J. Mater. Process. Technol. **182**, 637–643 (2007)
7. M. Azaouzi, H. Naceur, A. Delameziere, J.L. Batoz, S. Belouettar, An heuristic optimization algorithm for the blank shape design of high precision metallic parts obtained by a particular stamping process. Finite Eleme. Anal. Des. **44**, 842–850 (2008)
8. Kh. Khalili, P. Kahhal, E. Efthekhari Shahri, M.S. Khalili, Blank optimization in elliptical-shaped sheet metal forming using response surface model coupled by reduced basis technique and finite element analysis. Key Eng. Mater. **473**, 683–690 (2011)
9. Y. Huang, Z.Y. Lo, R. Du, Minimization of the thickness variation in multi-step sheet metal stamping. J. Mater. Process. Technol. **177**, 84–86 (2006)
10. T. Ohata, Y. Nakamura, T. Katayama, E. Nakamachi, Development of optimum process design system for sheet fabrication using response surface method. J. Mater. Process. Technol. **143–144**, 667–672 (2003)
11. W. Hu, L.G. Yao, Z.Z. Hua, Optimization of sheet metal forming processes by adaptive response surface based on intelligent sampling method. J. Mater. Process. Technol. **197**, 77–88 (2008)
12. T. Jansson, L. Nilsson, Optimizing sheet metal forming processes—using a design hierarchy and response surface methodology. J. Mater. Process. Technol. **178**, 218–233 (2006)
13. T. Jansson, A. Andersson, L. Nilsson, Optimization of draw-in for an automotive sheet metal part: an evaluation using surrogate models and response surfaces. J. Mater. Process. Technol. **159**, 426–434 (2005)
14. S. Guangyong, L. Guangyao, G. Zhihui, C. Xiangyang, Y. Xujing, L. Qing, Multiobjective robust optimization method for drawbead design in sheet metal forming. Mater. Des. **31**, 1917–1929 (2010)
15. A. Konak, D.W. Coit, A.E. Smith, Multi-objective optimization using genetic algorithms: a tutorial. Reliab. Eng. Syst. Saf. **91**, 992–1007 (2006)
16. A. Farhang-Mehr, S. Azarm, Entropy-based multi-objective genetic algorithm for design optimization. Struct. Multidiscipl. Optim. **24**, 351–361 (2002)
17. T. Hiroyasu, M. Miki, J. Kamiura, S. Watanabe, H. Hiroyasu, Multi-objective optimization of diesel engine emissions and fuel economy using genetic algorithms and phenomenological model. SAE paper no. 2002-01-2778 (2002)
18. E.M. Kasprzak, K.E. Lewis, Pareto analysis in multiobjective optimization using the collinearity theorem and scaling method. Struct. Multidiscipl. Optim. **22**, 208–218 (2001)
19. W. Liu, Y. Yang, Multi-objective optimization of sheet metal forming process using Pareto-based genetic algorithm. J. Mater. Process. Technol. **208**, 499–506 (2008)
20. W.F. Hosford, R.M. Caddel, *Metal Forming Mechanics and Metallurgy* (Cambridge University Press, Cambridge, 2007), Chap. 15, pp. 241–244